

6th Workshop on Metallization and Interconnection for Crystalline Silicon Solar Cells, 2016

## Single print metal stencils for high-efficiency PERC solar cells

H. Hannebauer<sup>a,\*</sup>, T. Falcon<sup>b</sup>, J. Cunnusamy<sup>b</sup>, T. Dullweber<sup>a</sup>

<sup>a</sup>Institute for Solar Energy Research Hamelin (ISFH), Am Ohrberg 1, D-31860 Emmerthal, Germany

<sup>b</sup>ASM Alternative Energy, 11 Albany Road, Weymouth, DT4 9TH, U.K.

### Abstract

Industrial silicon solar cells like Passivated Emitter and Rear Cells (PERC) typically apply a screen-printed (Ag) front contact with a single print process using a mesh screen. It has been shown that using stencils instead of screens improves the finger profile leading to slightly higher cell conversion efficiencies. However, so far stencil printing required an extra printing step for the busbars since conventional stencils do not support H-pattern designs. In this paper, we evaluate a novel “single print” stencil from ASM AE that allows to print busbars and fingers in a single print step. We apply the novel single print stencil to high-efficiency PERC solar cells and compare it to today’s industrial screen printing processes (single print and dual print) as well as to a high performance dual-printed front side grid applying a stencil for the fingers and a screen for the busbars. The printed finger width ranges from  $35.8 \pm 2.3 \mu\text{m}$  for  $30 \mu\text{m}$  stencil opening to  $46.7 \pm 3.4 \mu\text{m}$  for  $40 \mu\text{m}$  screen opening which leads to an  $0.5\%_{\text{abs}}$  increased metallized area on the front side of the screen printed fingers compared to the stencil printed fingers. The resulting average finger height is  $22.3 \mu\text{m}$  for the stencil groups and  $11.9 \mu\text{m}$  for the screen printed Ag finger which leads to a difference in the finger line resistance and an additional series resistance contribution for the screen-printed cells of  $0.05 \Omega\text{cm}^2$ . We achieve almost identical PERC cell efficiencies with the single print stencil and the dual print stencil process obtaining best values up to 21.1% and average values of 21.0%. In contrast, both screen printed groups achieve  $0.2\%_{\text{abs}}$  lower average conversion efficiencies mostly due to the lower  $J_{\text{sc}}$  and  $FF$ . The advantage of the dual print process compared to single print is shown in the increased  $V_{\text{oc}}$  by 1 to 2 mV due to the used non-firing through Ag busbar paste. With these results we demonstrate that the single print stencil process saves two process steps compared to dual print using a stencil while obtaining the same PERC cell performance with an efficiency gain of  $0.2\%_{\text{abs}}$  compared to today’s industrial screen print processes.

© 2016 The Authors. Published by Elsevier Ltd. This is an open access article under the CC BY-NC-ND license (<http://creativecommons.org/licenses/by-nc-nd/4.0/>).

Peer-review under responsibility of the organizing committee of the Metallization Workshop 2016

**Keywords:** Silicon solar cell; Stencil printing; Screen-printing; Metallization; Dual print; PERC;

\* Corresponding author. Tel.: +49-5151-999-637; fax: +49-5151-999-400.  
E-mail address: [hannebauer@isfh.de](mailto:hannebauer@isfh.de)

## 1. Introduction

Silicon solar cells like industrial-type Passivated Emitter and Rear Cells (PERC) typically apply a screen-printed silver (Ag) front contact with a single print process using a mesh screen [1]. Due to the strongly improved rear side of PERC cells [2], future efficiency increases are expected to originate from optimization of the front side grid [3,4]. The wire mesh in the finger aperture of a mesh screen reduces the open area to a typically value of 60% [5] which affects the obtainable finger height and homogeneity along the finger length. A promising alternative is stencil printing [6] which features 100% open finger area. This leads to a benefit of excellent paste transfer efficiency and hence improves the finger height and drastically reduces the finger roughness. The resulting PERC solar cells with stencil-printed fingers show reduced Ag paste consumption and increased efficiencies [7]. However, it is necessary to print the front grid in two consecutive printing steps (first busbars, then fingers) called “dual print” [8] since conventional stencils are not supporting H-pattern designs including fingers and busbars. Previous work on dual print with stencil printed contact finger demonstrated an efficiency up to 19.8% with an Ag paste consumption of 67.7 mg [9] as well as an efficiency of 21.2% with 74 mg Ag paste consumption applying a 5 busbar front grid [4]. To avoid the two additional and required process steps (printing and drying), there exist few prototypes of double layer stencils which can print the H-pattern in one printing step [8,10-12]. However, the open area in the finger aperture of these dual layer stencils is reduced to around 80% [8,11] due to bridges to keep the pattern together.

In this contribution, we report for the first time results using an industrially feasible single print dual layer stencil that enables to print busbars and fingers in a single process step and still features 100% open finger area. We apply the novel single print stencil to high-efficiency PERC solar cells and compare it to today’s industrial screen print processes as well as to a high performance dual-printed front side grid applying a stencil for the fingers and a screen for the busbars. We measure the resulting Ag paste consumption after printing before drying, the resistance contribution of the front metallization, and all IV parameters of the final PERC solar cells.

## 2. Impact of printing parameters on Ag paste consumption and front grid resistance

For the silver front side metallization we evaluate four split groups with different printing processes which are displayed in Table 1. The front grid layout has five busbars with a width of 0.5 mm per busbar. Dual print in groups 1 and 3 in Table 1 means that first the busbars are screen-printed with a non-firing through Ag paste C resulting in a paste consumption for the busbars of 14.2 mg after printing prior to drying. The subsequently applied finger print uses either a nickel stencil (group 1) or a mesh screen (group 3). The single print process applied to group 2 and group 4 prints the H-pattern front grid with fingers and busbars in one printing step. We calculate the optimal number of fingers using the equations from Mette [13]. Groups 1 and 2 use a stencil finger opening width of 30  $\mu\text{m}$  with 118 fingers per wafer, groups 3 and 4 use a screen finger opening width of 40  $\mu\text{m}$  with 109 fingers per wafer. A metal squeegee and R&D Ag paste A with high viscosity developed for stencil printing is used for finger print of both groups 1 and 2. The finger screen print in group 3 and 4 is done by using a polyurethane squeegee with shore hardness of 75A and commercially available silver paste B which is a state of the art screen-printing paste. Both Ag pastes A and B based on the same inorganic composition. These printing variations lead to a measured Ag paste consumption after printing prior to drying for the front side metallization between 74.1 mg and 112.8 mg as summarized in Table 1.

Table 1: Printing parameters and measured Ag paste consumption on PERC solar cells with five busbar layout for the four investigated split groups including the single print stencil.

Group	Printing technique	Type of Ag finger print	Ag finger aperture [ $\mu\text{m}$ ]	Ag paste	Finger paste consumption [mg]	Busbar paste consumption [mg]	Front Ag paste consumption [mg]
1	Dual Print	Stencil	30	A	86.0	14.2	100.2
2	Single Print	Stencil	30	A	-	-	112.8
3	Dual Print	Screen	40	B	59.9	14.2	74.1
4	Single Print	Screen	40	B	-	-	91.5

For the single print stencil process in group 2 we use a stencil prototype from ASM AE which is able to print the fingers as well as the busbars in one printing step. The single print stencil is a two layer metal foil, with each layer being fabricated by a separate photolithography and nickel electro-plating process. This results in a strong bond between the two layers of nickel, thereby forming a single foil. The completed foil is mounted in a re-usable spring-tensioned framing system which has the advantage of offering more precise and consistent control over the foil tension than a regular mesh mount stencil. The top (or squeegee side) layer of nickel has a mesh grid over the busbar regions as shown in Fig. 1. This layer is not full stencil thickness, instead the mesh layer acts as a bridge over the busbar region. The finger regions are 100% open (no top grid) and are fully stencil thickness, being defined by both nickel layers. Typically the full stencil thickness will be determined by the finger opening width in a ratio of approximately 1:1.

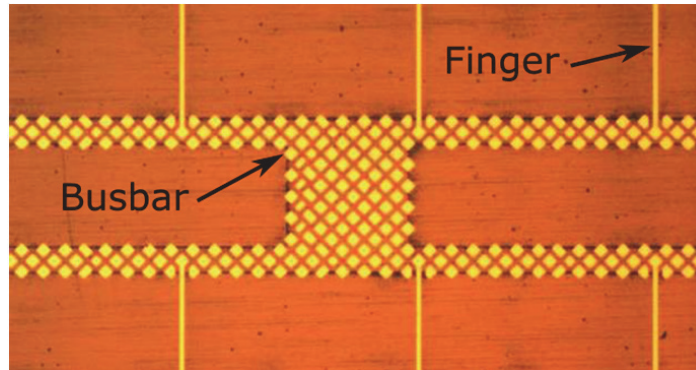


Fig. 1: Light microscope image of the single print stencil. The top layer of the stencil has a mesh grid over the busbar regions which acts as a bridge. The finger regions are 100% open and fully stencil thickness.

The finger profiles obtained with the different printing parameters are analyzed with a Wyko NT9100 optical profilometer. Images of the printed Ag fingers after firing of group 2 (stencil) and group 3 (screen) are displayed in Fig. 2 a) – b). The Ag finger of the other two groups look very similar compared to the displayed profiles for the same type of finger print (stencil/screen). We calculate the average finger height by measuring the finger profile over a finger length of 0.5 mm at the bottom, the mid, and the top of the cell between the busbars. The stencil printed finger has an average height of 22.3  $\mu\text{m}$  and high aspect ratio of 0.62 as well as a very homogeneous height along the finger due to the 100% open area in the aperture. In contrast, we measure an average finger height of only 11.9  $\mu\text{m}$  for the screen printed Ag finger with a difference of more than 11  $\mu\text{m}$  between the minimum and the maximum finger height. The printed finger width is measured by optical light microscope on eight positions for two cells of each group and ranges from  $35.8 \pm 2.3 \mu\text{m}$  for 30  $\mu\text{m}$  stencil opening to  $46.7 \pm 3.4 \mu\text{m}$  for 40  $\mu\text{m}$  screen opening.

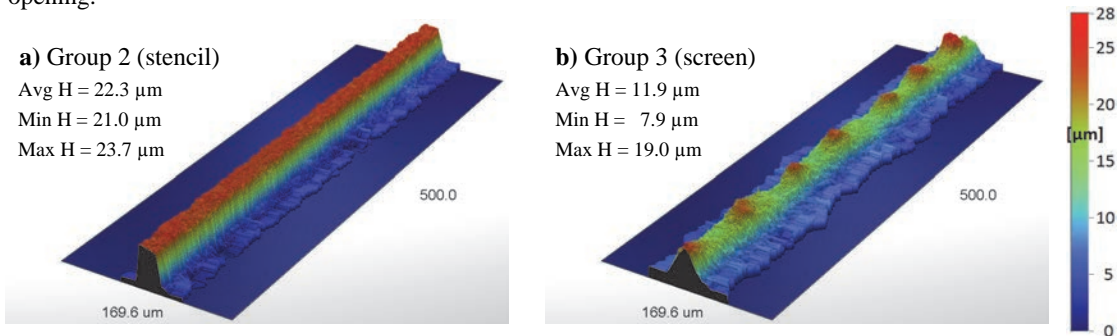


Fig. 2: Finger profiles measured with an optical profilometer printed using a) stencil in group 2 or b) mesh screen in group 3. “H” denotes the measured finger height.

In addition, we measure the finger line resistance  $r_L$  as well as the specific front contact resistance  $\rho_c$  to the emitter. For the finger line resistance, we measure the resistance between the busbars taking into account the distance between the busbars as well as the number of fingers. The lowest  $r_L$  of  $0.63 \pm 0.11 \Omega/\text{cm}$  is obtained for the stencil printed fingers of groups 1 and 2. The screen printed Ag fingers in groups 3 and 4 achieve a finger line resistance of  $1.06 \pm 0.04 \Omega/\text{cm}$ . This results in an additional series resistance contribution for the screen-printed groups of  $0.05 \Omega\text{cm}^2$ . The specific contact resistance is measured using the transfer length method TLM [14]. The measurement is done on 10 mm wide strips to ensure that the varying finger line resistance does not influence the TLM results. The PERC solar cells show an average  $\rho_c$  of  $2.26 \pm 0.76 \text{ m}\Omega\text{cm}^2$  for paste A and  $2.40 \pm 1.22 \text{ m}\Omega\text{cm}^2$  for paste B which leads to the same series resistance contribution of the contact resistance for all split groups.

### 3. PERC solar cells with different front grid processes

For PERC solar cell processing, we use  $2 \Omega\text{cm}$ ,  $156 \times 156 \text{ mm}^2$ , boron-doped Czochralski-grown silicon wafers. The process flow is described in detail in [2]. Here we just highlight the most important process steps. After cleaning and damage etching, the rear side is coated with a dielectric protection layer which acts as etching and diffusion barrier in the following alkaline texturing and phosphorus diffusion. The homogeneously doped emitter has a sheet resistance of  $105 \Omega/\text{sq}$ . After texturing and diffusion, the protection layer is removed by wet chemistry, followed by a cleaning step. The rear side is passivated by an atomic-layer-deposited (ALD)  $\text{Al}_2\text{O}_3/\text{SiN}_x$  layer stack, whereas the front side is covered with a PECVD  $\text{SiN}_x$  antireflective layer of thickness of about 70 nm. Then, the rear passivation is locally removed by laser ablation in order to form line-shaped rear contacts. After the full-area aluminium (Al) rear side print, we use an ASM AE Eclipse printer for the silver front side metallization and evaluate different printing processes as described in Table 1. A drying process in a belt furnace completes each printing step. The front and the rear contacts are fired in a conventional belt furnace during which the Al paste locally alloys with the silicon wafer at areas where the rear passivation has been removed by laser ablation.

A schematic drawing of the resulting PERC solar cell is shown in Fig. 3.

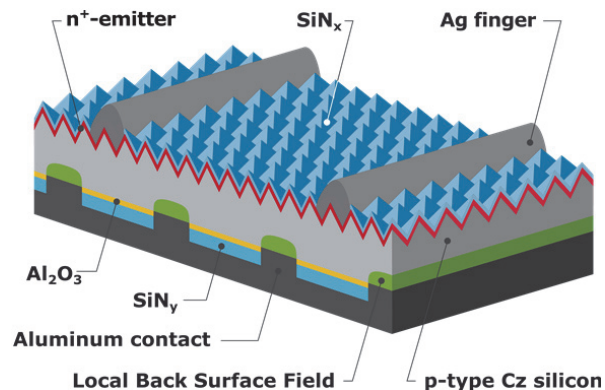


Fig. 3: Schematic drawing of the PERC silicon solar cell with printed Ag front and Al rear contacts.

Figure 4 shows the conversion efficiency  $\eta$  as well as the open-circuit voltage  $V_{oc}$ , the short-circuit current-density  $J_{sc}$ , and the fill factor  $FF$  of the resulting PERC solar cells of the four split groups. Each group consist of three identical processed solar cells. The results have been obtained at best firing conditions after an optimization. The PERC cells process with the single print stencil obtain almost identical PERC cell efficiencies with best values up to 21.1% and average values of 21.0% as the PERC cells process with dual print and stencil for the finger print. Both screen printed groups achieve slightly lower average conversion efficiencies of 20.8%. The influence of the non-firing through Ag paste used in the dual print processes is visible in the  $V_{oc}$  with a gain of 1 to 2 mV compared

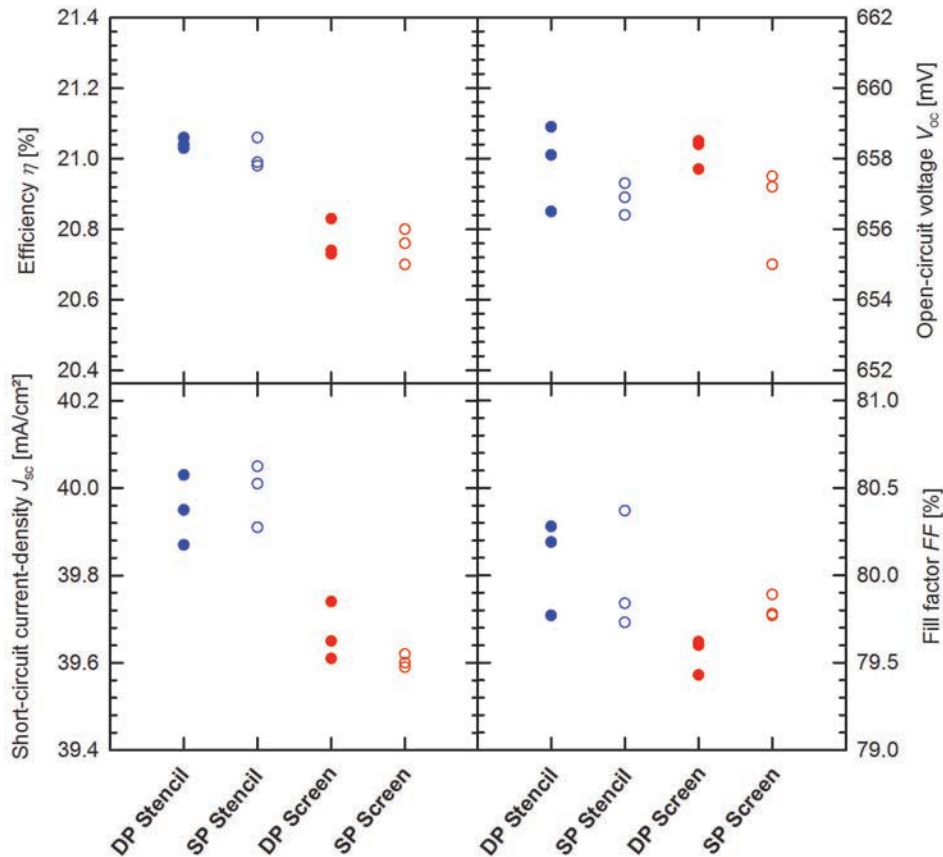


Fig. 4: Conversion efficiency  $\eta$ , open-circuit voltage  $V_{oc}$ , short-circuit current-density  $J_{sc}$ , and fill factor  $FF$  of PERC solar cells of four split groups with different printing processes according to Table 1.

to the single print processes. The slightly lower  $J_{sc}$  by 0.3 mA/cm<sup>2</sup> of the screen printed PERC cells compared to the stencil printed PERC cells is due to an 0.5%<sub>abs</sub> increased metallized area on the front side caused by the increased finger width of the screen printed fingers compared to the stencil printed fingers. Additionally, the average  $FF$  of the stencil printed groups 1 and 2 is 0.3%<sub>abs</sub> higher compared to groups 3 and 4 using a mesh screen for Ag fingers which is caused by the lower finger line resistance as well as lower emitter resistance due to higher number of fingers. In summary, the single print stencil obtains comparable PERC IV parameters as the dual print stencil and both processes slightly outperform the screen-printed process variants due to the narrower finger widths and more homogeneous finger profile of the stencil printed fingers.

#### 4. Conclusion

We applied the novel VectorGuard single print dual layer stencil from ASM AE to high-efficiency PERC solar cells and compare it to today's industrial screen print processes as well as to a high performance dual-printed front side grid. The average height of the stencil printed fingers is 22.3  $\mu\text{m}$  in contrast to 11.9  $\mu\text{m}$  with a mesh screen. This leads to a higher finger line resistance and an additional series resistance contribution for the screen-printed groups of 0.05  $\Omega\text{cm}^2$ . However, the specific contact resistance of the front side to the emitter is similar for the stencil paste A and screen print paste B. The resulting PERC solar cells demonstrate efficiencies up to 21.1% for

both stencil printed groups. In contrast, both screen printed groups achieve 0.2%<sub>abs</sub> lower average conversion efficiencies mostly due to a lower  $J_{sc}$  (larger finger width) and a lower  $FF$  (lower finger height). The dual print processes show a benefit in the  $V_{oc}$  with a gain of 1 to 2 mV compared to the single print processes due to the non-firing through Ag busbar paste and therefore reduced recombination in the emitter. Hence, we demonstrate that the single print stencil process saves two process steps compared to dual print using a stencil while obtaining the same PERC cell performance with an efficiency gain of 0.2%<sub>abs</sub> compared to today's industrial screen print processes.

## Acknowledgements

We thank the German Federal Ministry for Economic Affairs and Energy for funding part of this work under contract no. 0325753D (HighPERC).

## References

- [1] ITRPV Working Group. International Technology Roadmap for Photovoltaic, 2014 Results. April 2015
- [2] Dullweber T, Gatz S, Hannebauer H, Hesse R, Schmidt J, Brendel R. Towards 20% efficient large-area screen-printed rear-passivated silicon solar cells. *Prog Photovolt: Res Appl* **20**;2012:630-8.
- [3] Metz A, Adler D, Bagus S, Blanke H, Bothar M, Brouwer E, Dauwe S, Dressler K, Droessler R, Droste T, Fiedler M, Gassenbauer Y, Grahl T, Hermert N, Kuzminski W, Lachowicz A, Lauinger T, Lenck N, Manole M, Martini M, Messmer R, Meyer C, Moschner J, Ramspeck K, Roth P, Schönfelder R, Schum B, Sticksel J, Vaas K, Volk M, Wangemann K. Industrial high performance crystalline silicon solar cells and modules based on rear surface passivation technology. *Sol Energy Mater Sol Cells* **120**;2014:417-25.
- [4] Hannebauer H, Dullweber T, Baumann U, Falcon T, Brendel R. 21.2%-efficient fineline-printed PERC solar cell with 5 busbar front grid. *Phys Status Solidi RRL* **8** (8);2014: 675-9.
- [5] Falcon T. Ultra Fine Line Printing for Silicon Solar Cells....Mesh Screens or Metal Stencils? *Presentation at the 3rd Metallization Workshop*, Charleroi, Belgium, 2011.
- [6] de Moor H.H.C, Weeber A.W, Hoonstra J, Sinke W.C. Fine-line screen printing for silicon solar cells. *6th Colorado Workshop*, Snowmass, 1996, p. 154-170.
- [7] Hannebauer H, Schimanke S, Falcon T, Altermatt P.P., Dullweber T. Optimized stencil print for low Ag paste consumption and high conversion efficiencies. *Energy Procedia* **67**;2015:108–15.
- [8] Hoonstra J, Heurtault B. Stencil print applications and progress for crystalline silicon solar cells. *Proc 24th European Photovoltaic Solar Energy Conference*, Hamburg, Germany, 2009, p. 989-992.
- [9] Hannebauer H, Dullweber T, Falcon T, Chen X, Brendel R. Record low Ag paste consumption of 67.7 mg with dual print. *Proc 4th Metallization Workshop, Energy Procedia* **43**;2013:66-71.
- [10] Hoonstra J, Roberts S, de Moor H.H.C., Bruton T.M. First experiences with double layer stencil printing for low cost production solar cells. *2nd World PVSEC*, Vienna, 1998, p. 1527-1530.
- [11] Hoonstra J, de Moor H, Weeber A, Wyers P. Improved front side metallization on silicon solar cells with stencil printing. *Proc 16th European Photovoltaic Solar Energy Conference*, Glasgow, U.K., 2000, p. 1416-1419.
- [12] Falcon T. Aspect ratio improvements for printed frontside conductors on silicon solar cells. *Proc 24th European Photovoltaic Solar Energy Conference*, Hamburg, Germany, 2009, p. 1338-1346.
- [13] Mette A. New concepts for front side metallization of industrial silicon solar cells. PhD thesis, Freiburg, Germany, 2007.
- [14] Shockley W. Research and investigation of inverse epitaxial UHF power transistors. Report No. AI-TDR-64-207, AF Avionics Laboratory, Research and Technology Division, Air Force Systems Command. Wright-Patterson Air Force Base, Ohio, 1964.